ELSEVIER

Biophysical Chemistry 115 (2005) 77–85

Biophysical Chemistry

http://www.elsevier.com/locate/biophyschem

# Molecular dynamics simulations of evolved collective motions of atoms in the myosin motor domain upon perturbation of the ATPase pocket

Tatsuyuki Kawakubo[a,*], Okimasa Okada[b], Tomoyuki Minami[c]

[a]*Faculty of Engineering, Toin University of Yokohama, Aoba-ku,Yokohama 225-8502, Japan*
[b]*Optical System Business Development, Fuji Xerox Co., Ltd., Nakai-machi, Kanagawa 259-0157, Japan*
[c]*Science Systems, Industrial Materials and Products Div., Fuji Photo Film Co., Ltd., Minato-ku, Tokyo 106-8620, Japan*

Received 28 September 2004; received in revised form 24 December 2004; accepted 24 December 2004
Available online 28 January 2005

**Abstract**

A crucial point for mechanical force generation in actomyosin systems is how the energy released by ATP hydrolysis in the myosin motor domain gives rise to the movement of the myosin head along the actin filament. We assumed the signal of the ATP hydrolysis to be transmitted as modulated atomic vibrations from the nucleotide-binding site throughout the myosin head, and carried out 1-ns all-atom molecular dynamics simulations for that signal transmission. We distributed the released energy to atoms located around the ATPase pocket as kinetic energies and examined how the effect of disturbance extended throughout the motor domain. The result showed that the disturbance signal extended over the motor domain in 150 ps and induced slowly varying collective motions of atoms at the actin-binding site and the junction with the neck, both of which are relevant to the movement of the myosin head along the actin filament. We also performed a principal component analysis of thermal atomic motions for the motor domain, and the first principal component was consistent with the response to the disturbance given to the ATPase pocket.


*Keywords:* Molecular dynamics (MD) simulation; Myosin motor domain; ATP hydrolysis; Collective intra-molecular motions of atom; Principal component analysis

## 1. Introduction

At the molecular level, muscle contraction is caused by movement of the myosin head relative to the actin filament. This movement is triggered by ATP hydrolysis, which occurs in the ATPase pocket within the motor domain of myosin heads. Two models have been presented for this chemo-mechanical coupling: the lever-arm model [1] and the loose-coupling model [2]. In the lever-arm model, the myosin head repeatedly attaches to and detaches from the actin filament via conformational changes and then flips forward along the filament. From crystallographic analyses of myosin heads complexed with nucleotide analogues, the conformational changes of the myosin head are assumed to strongly couple with each step of ATP hydrolysis, with one-to-one correspondence [3–6]. On the other hand, the loose-coupling model is based on fluorescence microscopy of single molecular motions [7], and the movement of the myosin head relative to the actin filament during the hydrolysis of a single ATP encompasses multiple steps that are not always in the forward direction. Thus, in the loose-coupling model, the movement of the myosin head is considered to be analogous to directed Brownian motion [2].

The actin-binding site and the junction site with the neck are both several nanometers away from the ATPase pocket in the myosin head, so that an issue of how the signal of the ATP hydrolysis could be transmitted from the nucleotide-binding site to the two sites has been of great interest [1]. A widely accepted view was that the force

* Corresponding author. Tel.: +81 45 974 5058; fax: +81 45 972 5972.
*E-mail address:* tatsu@cc.toin.ac.jp (T. Kawakubo).

0301-4622/$ - see front matter © 2005 Elsevier B.V. All rights reserved.
doi:10.1016/j.bpc.2004.12.049

generation was caused by a release of the bound nucleotide from the myosin head and molecular dynamics (MD) simulations were carried out to examine a conformational change involved in the route of phosphate release following ATP hydrolysis [8,9]. On the other hand, simultaneous measurements of the release of nucleotide and the mechanical reaction of a single myosin by Yanagida's group [10] revealed that the mechanical reaction started regardless of the release of the nucleotide and surprisingly in some cases the former preceded the latter. Thus in the present work, we regarded a modification of atomic vibrations due to a disturbance of the ATP hydrolysis as a candidate of the event signal. We assumed that the energy released by ATP hydrolysis is transformed into kinetic energy of atoms located around the ATPase pocket in the motor domain [11] and examined how its effect spread over the motor domain through atomic interactions using all-atom MD simulations.

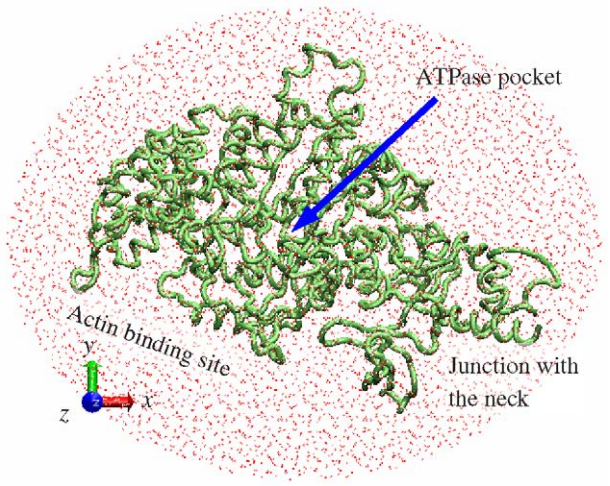


Fig. 2. Backbone structure of the motor domain of myosin solvated with a spheroidal water droplet. The coordinates $x$, $y$ and $z$ are defined as follows: their origin is taken at the center of the spheroidal water droplet and the $x$ axis is defined in the horizontal direction, the $y$ axis in the vertical direction, and the $z$ axis is perpendicular to the $x$–$y$ plane.

## 2. Procedure of MD simulations

From the structure data of myosin subfragment-1 S1 from scallop (PDB; 1kk7, M. Himmel et al.), we took the motor domain (the N-terminal 785 residues) and repaired missing residues in the original data. In Fig. 1, the structure of S1, including an ATP analog (PDB; 1kk8, M. Himmel et al.), delineates the position of the ATPase pocket. The motor domain with a long and narrow shape was solvated with a spheroidal water droplet as shown in Fig. 2, so as to reduce the amount of calculation. The soft half-harmonic potential [12] was applied to prevent the water molecules from evaporating. The initial distance from the motor domain to the soft half-harmonic potential wall was more than 10 Å. The whole system comprising polypeptides and water was thermally equilibrated at 300 K for 300 ps. The total number of atoms is 68,662. After this process, the trajectories of each atom were calculated under the following two different initial conditions.

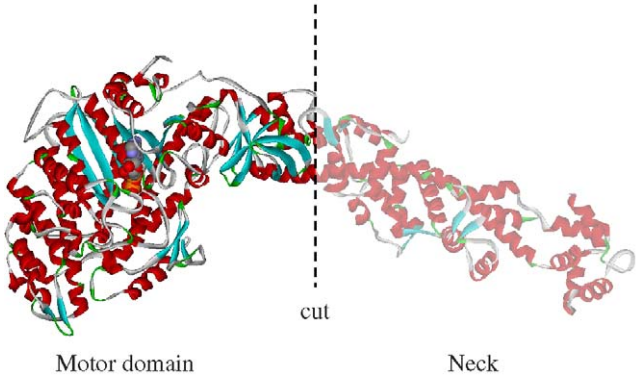


Fig. 1. A ribbon diagram of the scallop S1 structure (PDB-1kk8) including an ATP analog, which is represented by a space-filling model within the motor domain. The myosin head was truncated along the broken vertical line, and the motor domain (left) was used for MD simulations.

1. Without giving any disturbance to the whole system, we continued to calculate the trajectories for additional 1 ns at 300 K.
2. An energy of $8.60\times10^{-20}$ J released by hydrolysis of one ATP molecule was distributed to 80 backbone atoms as kinetic energy by giving an additional velocity to each atom proportionally to its instantaneous velocity after the equilibration run without changing the direction. These atoms are located within a 10-Å radius around a position where the γ-phosphate would occupy when the myosin binds a nucleotide. Out of 80 atoms, 29 belong to the p-loop, 40 to switch I, and 11 to switch II. After giving the disturbance, MD calculations were carried out for 1 ns at 300 K.

Details of the calculations are as follows. The software was SANDER module in AMBER 7 [12]. We used AMBER force field with parm96 parameters [13] and the TIP3P [14] model for explicit water molecules. We have used a special purpose computer called MD EngineIIPC (Fuji Xerox Co., Ltd., Japan), which enables us to calculate the electrostatic interaction of every atomic pair without using the cut-off method. The van der Waals interaction was estimated using a cut-off distance of 15 Å. The time step of 2 fs was used with the SHAKE algorithm [15]. Berendsen's method [16] was used for temperature regulation during the initial thermal equilibration. However, the temperature was not regulated during the sampling runs with different initial conditions mentioned above to investigate the time evolution of the structural difference caused by the additional energy imitating the ATP hydrolysis. The graphical representations were prepared with VMD [17] and ViewerLite (Accelrys Inc., San Diego, CA, USA).

## 3. Results and discussion

### 3.1. Difference between trajectories of each atom with and without initial disturbance

Fig. 3 shows trajectories of α carbons in four representative residues under two different initial conditions. The blue line in each graph represents the trajectories without a disturbance and the red line the trajectories following a small disturbance that was initially given to 80 atoms in the ATPase pocket. As for the coordinates $x$, $y$ and $z$ denoted in Fig. 3, their origin was defined as the center of the spheroidal water droplet shown in Fig. 2; the $x$ axis was defined in the horizontal direction, the $y$ axis in the vertical direction, and the $z$ axis was perpendicular to the $x$–$y$ plane. The trajectory of residue 243, which is located in the ATPase pocket, was unaffected by the difference between two initial conditions. On the other hand, residues 368 and 541, which are located at the tips of two capes of the so-called actin-binding cleft [6], show remarkable differences

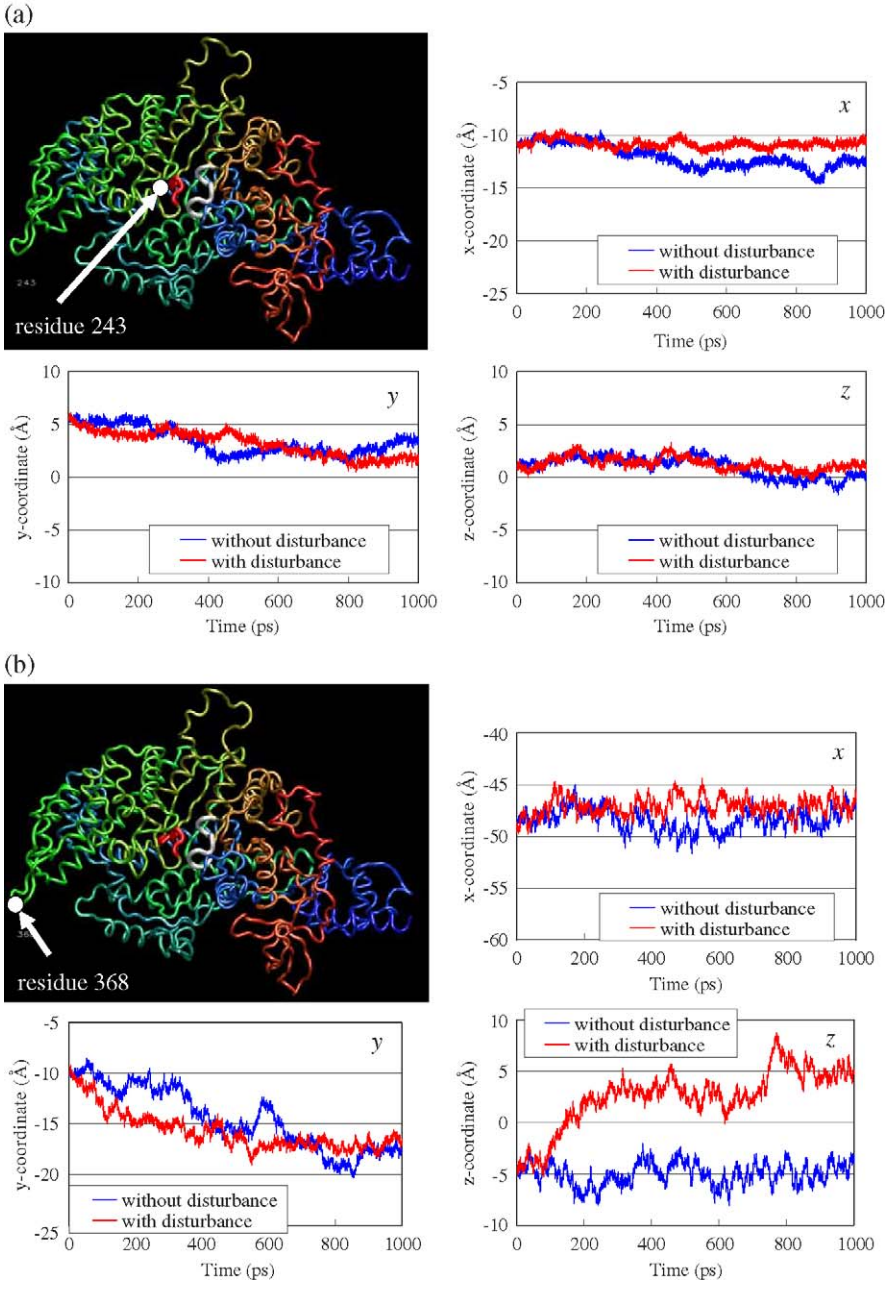


Fig. 3. The $x$, $y$ and $z$ components of trajectories for α carbons in four representative residues computed under two initial conditions: in the presence (red line) and absence (blue line) of a disturbance corresponding to ATP hydrolysis. The image at the top-left in each figure shows the position of the relevant residue. (a) Residue 243 is located at the switch I region in the ATPase pocket; (b) residue 368 and (c) residue 541 are located in the upper and lower 50-kDa subdomains, respectively; and (d) residue 722 is at the junction with the neck.

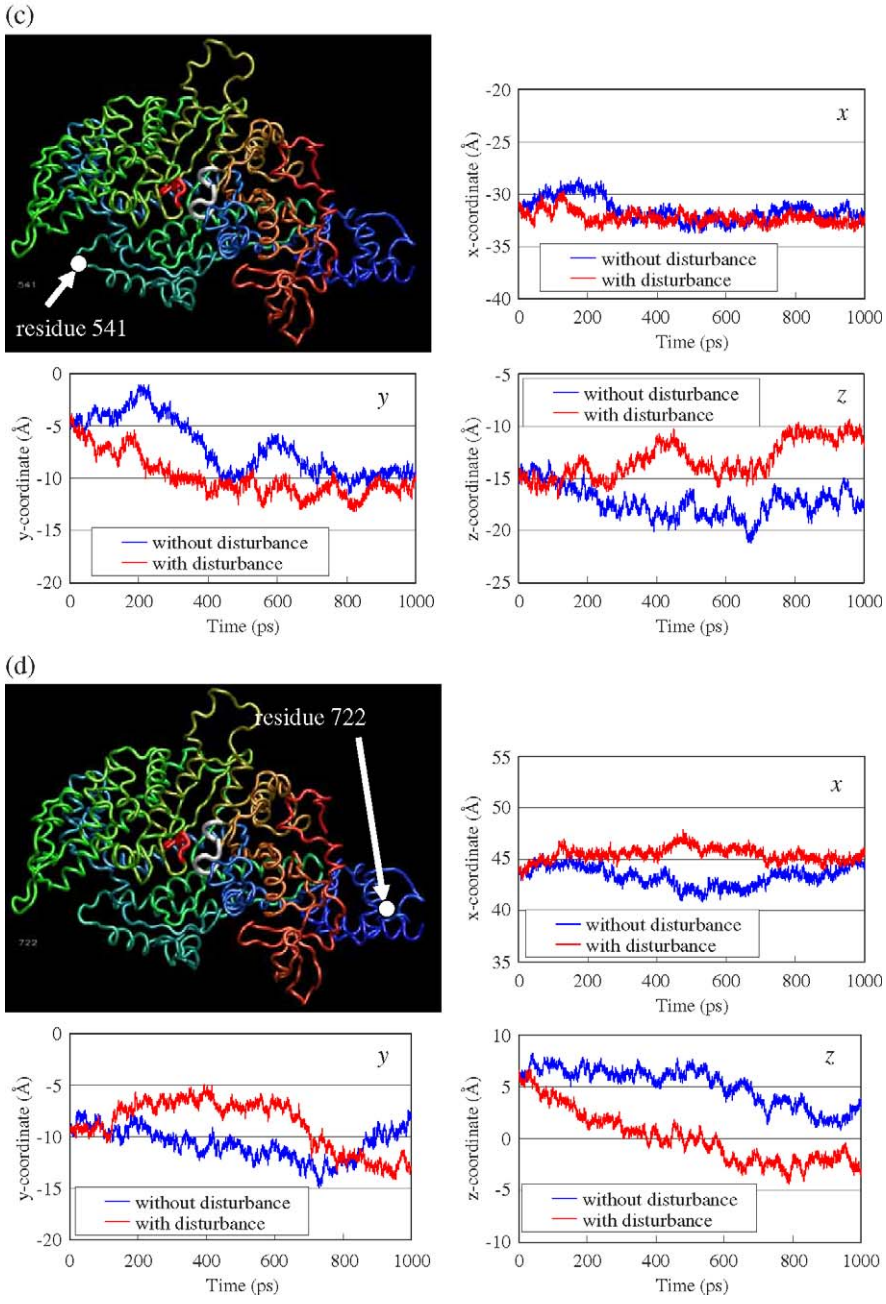


Fig. 3 (*continued*).

especially for the *y* and *z* coordinates. This was also the case for residue 722, which is located at the junction with the neck.

An X-ray diffraction analysis of the actomyosin complex from rabbit skeletal muscle fibers [18] showed that the diffraction pattern of the actin-based layer in the presence of ATP was strikingly diffuse compared with the rigor state in the absence of ATP. This result suggests that the atoms at the actin-binding site of S1 molecules move randomly in the presence of ATP. Large deviations of our MD trajectories for residues 368 and 541 due to the initial disturbance given to the ATPase pocket may be consistent with the results of the X-ray diffraction analysis. On the other hand, flush-induced phosphorescence anisotropy decay measurements revealed that myosin heads [19], and specifically the regulatory light chain (RLC) [20] in myofibrils, rotate over a wide range of angles in the presence of ATP, though they are immobilized in the rigor state without ATP. An electron paramagnetic resonance (EPR) spectrum of the isolated spin-labeled RLC of myosin [21] also showed nanosecond rotational motion within the RLC, which was eliminated when the RLC was bound to myosin heads in myofibrils or fibers in the rigor state. Furthermore, an analysis of X-ray solution scattering data [22] indicates that a conformational change of S1 in the

presence of MgATP is caused by a hinge-like bending between the motor domain and the neck. The large deviations appearing in the $y$ and $z$ coordinates of residue 722 in Fig. 3(d) may correspond to the bending or rotation of the motor domain relative to the neck, as indicated in the previous experiments [19–22].

### 3.2. Comparison of root mean square fluctuations of atomic positions obtained from MD simulations and from Debye–Waller factors

The root mean square (rms) fluctuations of atomic positions calculated by MD simulations can be compared with the Debye–Waller factors derived from X-ray analyses (PDB; 1kk7, M. Himmel et al.). Fig. 4(a) shows rms fluctuations of atomic positions of α carbons versus residue number obtained from the MD simulation over 1 ns in thermal equilibrium at 300 K (blue) and those in the case where an initial disturbance was added to the ATPase pocket (red). For comparison with experimental results, the rms fluctuations of atomic positions obtained from the Debye–Waller factors in the PDB-1kk7 data are shown in Fig. 4(b). The colored horizontal bar in (b) classifies the secondary structures of the main chain: red, light blue, black and yellow denote α helices, β sheets, other structures and missing residues, respectively. The atomic position of missing residues could not be determined, probably due to large thermal fluctuations; hence, there were no data for the Debye–Waller factors. For these missing residues, atomic positional fluctuations in the MD simulations were enhanced in the non-equilibrium state

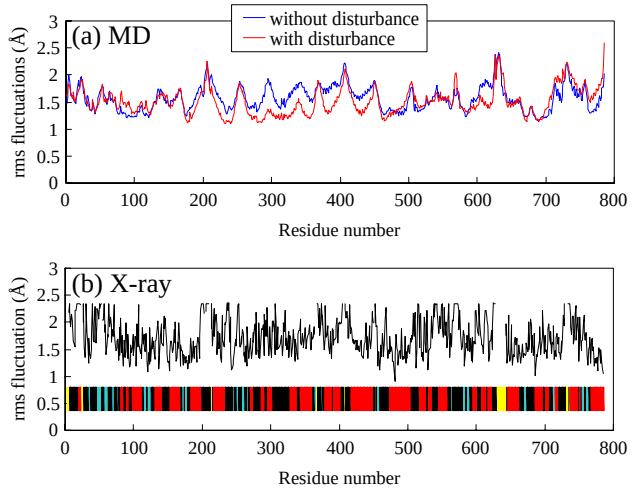


Fig. 4. Comparison among the root mean square (rms) fluctuations of atomic positions versus residue number: (a) obtained from 1 ns MD simulations in thermal equilibrium (blue) and from those following an initial disturbance (red); and (b) the rms fluctuations given in the crystallographic data of PDB-1kk7. The colored horizontal bar in (b) classifies the secondary structures of the main chain: the red, light blue, black and yellow denote α helices, β sheets, other structures and missing residues, respectively.

triggered by the disturbance as well as in the thermal equilibrium state.

### 3.3. Global evolution of coordinate deviations triggered by a small disturbance into collective motions of atoms

The preceding section presented the root mean square fluctuations of each atomic position averaged over 1 ns. Fig. 5 shows that coordinate deviations, triggered by a small disturbance given to atoms around the ATPase pocket, evolved into collective low frequency modes spreading over the motor domain. The abscissa represents the residue number and the ordinates $\Delta x$, $\Delta y$ and $\Delta z$ are the deviations of $x$, $y$ and $z$ coordinates of α carbons due to the initial disturbance from the coordinates in the absence of the disturbance at each time. The oblique line is the time axis. The time domains are separated into two parts: 0–1 ps (a, b, c) and 0–1000 ps (a′, b′, c′). The initial disturbance was given to three groups of atoms, i.e., the atoms of residues 174–184 (p-loop), 230–244 (switch I) and 460–463 (switch II). Effects of the disturbance appear as very small signals at a time of 0.05 ps in Fig. 5(a)–(c). At early times, each α carbon moves randomly irrespective of its neighbors, but slowly varying collective motions are grown up at around 150 ps. The influence of the disturbance spreads rapidly over the motor domain, due presumably to the multiplicity of folded structures of the protein and anharmonicities of the atomic interactions.

The motor domain is divided into four sub-domains, namely the N-terminal, the upper 50 kDa, the lower 50 kDa, and the converter, which roughly correspond to residues 1–175, 176–450, 451–707 and 708–785, respectively. Residues 601–670 in the third group are exceptional in that they belong to the upper 50-kDa sub-domain. According to Fig. 5(a′), almost all the atoms in the N-terminal, the upper 50-kDa and the converter sub-domains shift in the positive direction of $x$. In Fig. 5(b′), the atoms in the N-terminal and the converter sub-domains shift the $y$ component of deviations from positive to negative, which may indicate oscillatory behavior of the deviations. Fig. 5(c′) represents a noticeable aspect in that the actin-binding sites of residues 350–440 in the upper 50-kDa sub-domain and of residues 515–600 in the lower 50-kDa sub-domain deviate toward the positive direction of $z$, whereas the converter sub-domain (708–785) deviates toward the negative direction. These results indicate that the disturbance has a tendency to cause large atomic deviations at the N-terminal sub-domain, the actin-binding site and the converter sub-domain connected to the neck.

According to the linear response theory for a system, which is subjected to a generalized force or a disturbance, its response has a correlation with the thermal equilibrium fluctuations of the system. In order to check this correlation for the present system, we compared the root

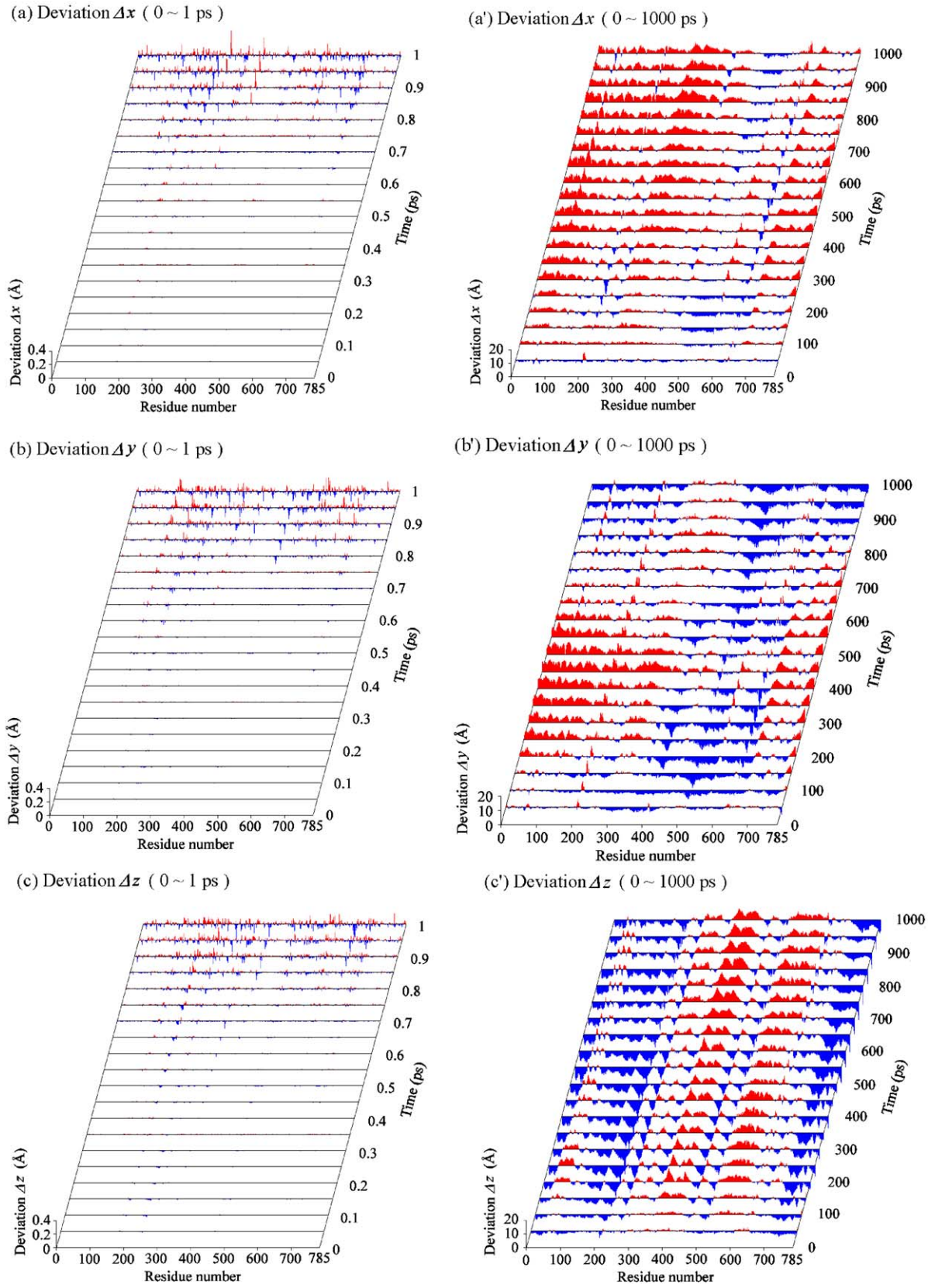


Fig. 5. Global evolution of coordinate deviations into collective modes spreading over the motor domain. Small coordinate deviations are initially triggered by a disturbance given to atoms around the ATPase pocket. The abscissa is the residue number and the ordinates $\Delta x$, $\Delta y$ and $\Delta z$ denote the deviations of the $x$, $y$ and $z$ coordinates of atoms following an initial disturbance from those in thermal equilibrium at each time. The oblique line is the time axis. The time domains are separated into two parts: 0–1 ps (a, b, c) and 0–1000 ps (a′, b′, c′).

mean square of the deviations of atomic positions with the rms fluctuations of atomic positions in thermal equilibrium. Fig. 6 shows their superimposed residue dependencies, which are found to be in accord with each other. This indicates that the linear response theory would be valid for dynamical response to a chemical disturbance in the myosin motor domain.

The energy utilized to drive the myosin head into interactions with the actin filament will not be sustained in a high frequency form such as thermal vibrations. This is likely to proceed in a form of low frequency collective modes. Previous stochastic theories and simulations, which are concerned with random motions of the myosin head along the actin filament (potentials for which are periodic but asymmetric), revealed that directed movements of the myosin head occur when the height of potentials fluctuates at some optimal frequency [23,24]. However, a full understanding of the random but directed movements will require large MD simulations that cover a thousand times longer period and account for all the interactions among atoms in both the myosin head and the actin filament.

### 3.4. Principal component analysis of thermal motions

The principal component analysis (PCA) of thermal motions is useful for predicting the most probable conformational deformation of proteins [25–27]. For the myosin head, collective mode analysis of overall structural fluctuations has been performed using a coarse-grained model to compare with X-ray solution scattering data [28]. We have carried out the PCA for the myosin motor domain, using all-atom MD thermal trajectories. After translational and rotational motions are removed, the variance–covariance matrix ($\sigma_{ij}$) of fluctuations of the three-dimensional coordinates $q_i$ ($i$=1–3 $N$; $N$=785) of the α carbons is calculated by,

$$\sigma_{ij} = \langle (q_i - \langle q_i \rangle)(q_j - \langle q_j \rangle) \rangle, \quad (1)$$

where <...> represents the average over 1 ns. The eigenvalues and eigenvectors are obtained by diagonalizing the variance–covariance matrix. The quasi-harmonic frequencies and quasi-harmonic modes of vibration are calculated from the eigenvalues and eigenvectors, respectively. The mode with largest eigenvalue is the first principal component, which corresponds to the slowest and most probable mode of atomic random motions.

The $x$–$y$ and $x$–$z$ plane projections of the first principal component are shown in Fig. 7. In order to depict the length and direction of the principal components in two-dimension, we have employed a method introduced by Tai K. et al. [28]. Each cone depicts the direction and the relative magnitude of the first principal component of fluctuations for each atom. The color of the cones indicates the magnitude of the vector changing from orange (long) to blue (short). Remarkable deviations are found at the N-terminal sub-domain, the actin-binding site and the converter sub-domain. This is consistent with the response to disturbance described in the Section 3.3. The residue number dependence of the magnitude of the first principal component (data not shown) was found to be roughly in accord with the blue curve in Fig. 4(a), which is the total rms fluctuations in thermal equilibrium. The relative contribution of the first principal component was 58%, implying that most of all the total fluctuations of atoms are expressed in terms of the first principal component.

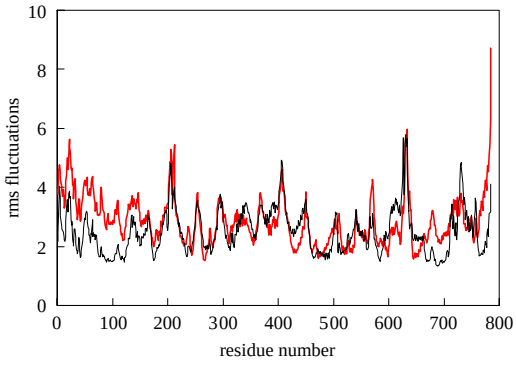


Fig. 6. Comparison of the rms fluctuations of (1) the atomic positions in thermal equilibrium (black) and (2) the deviations of atomic positions due to the disturbance (red).

For some protein functions, the problem will be reduced to addressing what kinds of collective modes are excited when some stimulation or disturbance is applied to the protein. Thus, mode analyses of fluctuations using MD simulations will be useful to examine the most probable inter-mode transfer of vibrational energy and to find a collective mode that is representative of protein function [29].

## 4. Conclusions

The run time of 1 ns is too short to describe the overall behavior of the myosin motor following an ATP hydrolysis. Our simulations, however, revealed that the signal of the ATP hydrolysis could be transmitted in 150 ps from the nucleotide-binding site throughout the motor domain. This is probably due to the multiplicity of folded structures of the protein and anharmonicities of the atomic interactions. Another point is that the disturbance given to the ATPase pocket was found to induce slowly varying collective motions of atoms at the actin-binding site and the junction with the neck, which are relevant to the sliding motion of the myosin head. In a relation to the linear response theory, the response to the disturbance was strongly correlated with the thermal equilibrium fluctuations of the atomic positions. Further, the first component of molecular motions obtained from the principal component analysis was also

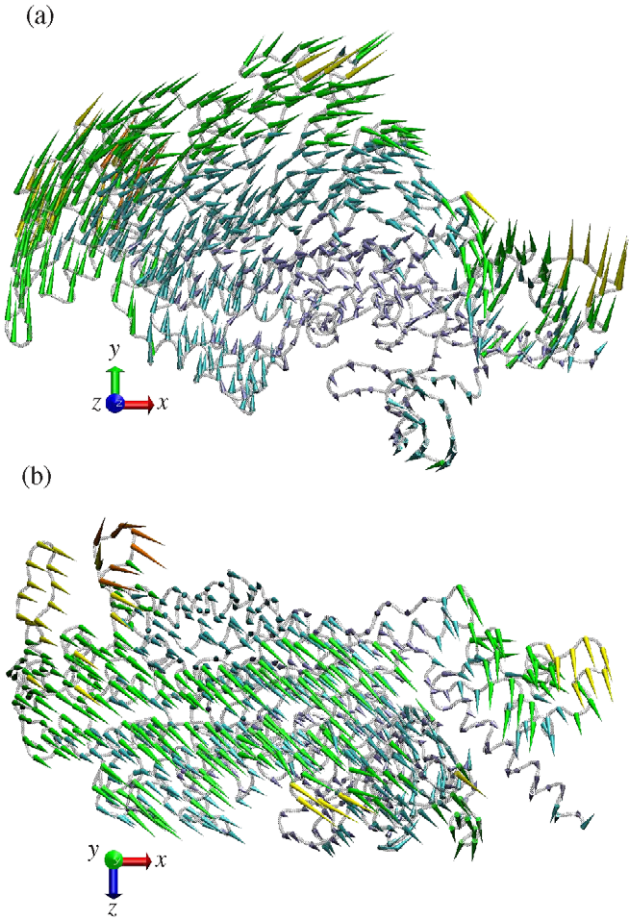


Fig. 7. Schematic representation of the eigenvector of the first principal component obtained from the thermal equilibrium MD simulation over 1 ns. Projections of the eigenvector are onto the *x*–*y* plane (a) and the *x*–*z* plane (b). Displacements of atoms are amplified so as to be clearly visible. The color of the cones indicates the magnitude of the vector changing from orange (long) to blue (short).

consistent with the response to the perturbation of the ATPase pocket.

## Acknowledgments

The authors would like to express their hearty thanks to Dr. M. Tsuda and Prof. K. Wakabayashi for useful discussions.

## Appendix A. Supplementary data

Supplementary data associated with this article can be found, in the online version, at doi:10.1016/j.bpc.2004.12.049.

## References

[1] J.A. Spudich, How molecular motors work, Nature 372 (1994) 515–518.
[2] T. Yanagida, S. Esaki, A.H. Iwane, Y. Inoue, A. Ishijima, K. Kitamura, T. Tanaka, M. Tokunaga, Single-motor mechanics and models of the myosin motor, Philos. Trans. R. Soc. Lond., B 355 (2000) 441–447.
[3] I. Rayment, H.M. Holden, M. Whittaker, C.B. Yohn, M. Lorenz, K.C. Holmes, R.A. Milligan, Structure of the actin–myosin complex and its implications for muscle contraction, Science 261 (1993) 58–65.
[4] Y. Suzuki, T. Yasunaga, R. Ohkura, T. Wakbayashi, K. Sutoh, Swing of the lever arm of a myosin motor at the isomerization and phosphate-release steps, Nature 396 (1998) 380–383.
[5] A. Houdusse, V.N. Kalabokis, D. Himmel, A.G. Szent-Györgyi, C. Cohen, Atomic structure of scallop myosin subfragment S1 comlexed with MgADP: a novel conformation of the myosin head, Cell 97 (1999) 459–470.
[6] D.M. Himmel, S. Gourinath, L. Reshetnikova, Y. Shen, A.G. Szent-Györgyi, C. Cohen, Crystallographic findings on the internally uncoupled and near-rigor states of myosin: further insights into the mechanics of the motor, Proc. Natl. Acad. Sci. 99 (2002) 12645–12650.
[7] K. Kitamura, M. Tokunaga, A.H. Iwane, T. Yanagida, A single myosin head moves along an actin filament with regular steps of 5.3 nanometres, Nature 397 (1999) 129–134.
[8] T.J. Minehardt, R. Cooke, E. Pate, P.A. Kollman, Molecular dynamics study of the energetic, mechanic, and structural implications of a closed phosphate tube in ncd, Biophys. J. 80 (2001) 1151–1168.
[9] J.D. Lawson, E. Pate, I. Rayment, R.G. Yount, Molecular dynamics analysis of structural factors influencing back door $P_i$ release in myosin, Biophys. J. 86 (2004) 3794–3803.
[10] A. Ishijima, H. Kojima, T. Funatsu, M. Tokunaga, H. Higuchi, H. Tanaka, T. Yanagida, Simultaneous observation of individual ATPase

and mechanical events by a single myosin molecule during interaction with actin, Cell 92 (1998) 161–171.
[11] R.D. Vale, F. Oosawa, Protein motors and Maxwell's demons: does mechanochemical transduction involve a thermal ratchet, Adv. Biophys. 26 (1990) 97–134.
[12] D.A. Case, D.A. Pearlman, J.W. Caldwell, T.E. Cheatham III, J. Wang, W.S. Ross, C.L. Simmerling, T.A. Darden, K.M. Merz, R.V. Stanton, A.L. Cheng, J.J. Vincent, M. Crowley, V. Tsui, H. Gohlke, R.J. Radmer, Y. Duan, J. Pitera, I. Massova, G.L. Seibel, U.C. Singh, P.K. Weiner, P.A. Kollman, AMBER, vol. 7, University of California, San Francisco, 2002.
[13] W.D. Cornell, P. Cieplak, C.I. Bayly, I.R. Gould, K.M. Merz Jr., D.M. Ferguson, D.C. Spellmeyer, T. Fox, J.W. Caldwell, P.A. Kollman, A second generation force field for the simulation of proteins, nucleic acids, and organic molecules, J. Am. Chem. Soc. 117 (1995) 5179–5197.
[14] W.L. Jorgensen, J. Chandrasekhar, J. Madura, M.L. Klein, Comparison of simple potential functions for simulating liquid water, J. Chem. Phys. 79 (1983) 926–935.
[15] J.-P. Ryckaert, G. Ciccotti, H.J.C. Berendsen, Numerical integration of the Cartesian equations of motion of a system with constraints: molecular dynamics of *n*-alkanes, J. Comput. Phys. 23 (1977) 327–341.
[16] H.J.C. Berendsen, J.P.M. Postma, W.F. van Gunsteren, A. DiNola, J.R. Haak, Molecular dynamics with coupling to an external bath, J. Chem. Phys. 81 (1984) 3684–3690.
[17] H. Iwamoto, K. Oiwa, T. Suzuki, T. Fujisawa, X-ray diffraction evidence for the lack of stereospecific protein interactions in highly activated actomyosin complex, J. Mol. Biol. 305 (2001) 863–874.
[18] S. Ishiwata, K. Kinoshita, H. Yoshimura, A. Ikegami, Rotational motions of myosin heads in myofibril studied by phosphorescence anisotropy decay measurements, J. Biol. Chem. 262 (1987) 8314–8317.
[19] S. Ramachandran, D.D. Thomas, Rotational dynamics of the regulatory light chain in scallop muscle detected by time-resolved phosphorescence anisotropy, Biochemistry 38 (1999) 9097–9104.
[20] O. Roopnarine, A.G. Szent-Györgyi, D.D. Thomas, Microsecond rotational dynamics of spin-labeled myosin regulatory light chain induced by relaxation and contraction of scallop muscle, Biochemistry 37 (1998) 14428–14436.
[21] Y. Sugimoto, M. Tokunaga, Y. Takezawa, M. Ikebe, K. Wakabayashi, Conformational changes of the myosin heads during hydrolysis of ATP as analyzed by X-ray solution scattering, Biophys. J. 68 (1995) 29s–34s.
[22] R.D. Astumian, M. Bier, Fluctuation driven ratchets, Phys. Rev. Lett. 72 (1994) 1766–1769.
[23] S. Esaki, Y. Ishii, T. Yanagida, Model describing the biased Brownian movement of myosin, Proc. Jpn. Acad., Ser. B 79 (2003) 9–14.
[24] N. Go, A theorem on amplitudes of thermal atomic fluctuations in large molecules assuming specific conformations calculated by normal mode analysis, Biophys. Chem. 35 (1990) 105–112.
[25] A. Kitao, F. Hirata, N. Go, The effects of solvent on the conformation and the collective motions of protein: normal mode analysis and molecular dynamics simulations of melittin in water and in vacuum, Chem. Phys. 158 (1991) 447–472.
[26] B.R. Brooks, D. Janežič, M. Karplus, Harmonic analysis of large systems. I: methodology, J. Comput. Chem. 16 (1995) 1522–1542.
[27] J. Higo, Y. Sugimoto, K. Wakabayashi, H. Nakmura, Collective motions of myosin head derived from backbone molecular dynamics and combination with X-ray solution scattering data, J. Comput. Chem. 22 (2001) 1983–1994.
[28] K. Tai, T. Shen, R.H. Henchman, Y. Bourne, P. Marchot, J.A. McCammon, Mechanism of acetylcholinesterase inhibition by fasciculin: a 5-ns molecular dynamics simulation, J. Am. Chem. Soc. 124 (2002) 6153–6161.
[29] K. Moritsugu, O. Miyashita, A. Kidera, Temperature dependence of vibrational energy transfer in a protein molecule, J. Phys. Chem., B 107 (2003) 3309–3317.